The role of organic compounds in artificial saliva for corrosion studies: evidence from XPS analyses.

Deborah Biggio[1], M. Fantauzzi[1], B. Elsener[1], D. Atzei[1], A. Rossi[1,*]
[1] *Dipartimento di Scienze Chimiche e Geologiche, Università di Cagliari, 09042 Cagliari, Italy.*

Keywords: surface chemistry, thin layer, brass, corrosion, saliva solutions.

Abstract

Several formulations of artificial saliva have been used for corrosion studies. The present work focuses on the effect of different saliva formulations on the composition of the surface film formed on CuZn37 brass alloy by X-ray photoelectron spectroscopy (XPS), in order to clarify the corrosion mechanism of historical brass wind instruments when used. Three different saliva solutions, Darvell (D), Carter-Brugirard (C-B) and SALMO, were selected. They differ for the content of the organic compounds. The XPS results show that on the brass exposed to C-B and SALMO the growth of a film made of CuSCN and zinc-phosphate is observed. In the case of samples exposed to D formulation, the only one that contains organic ligands, phosphorus is not revealed, a decrease in the zinc content in the film is detected and the S 2p shows the presence of a second component together with the one ascribed to CuSCN. A comparison with the results obtained on the pure metals in the presence of the organic compounds suggests that the formation of zinc and copper complexes may lead to thin and less protective surface film and thus to the observed high corrosion rates.

Introduction

Several formulations of artificial saliva have been proposed for electrochemical studies on alloys used in orthodontics. Human saliva is complex and its composition is unstable and strongly variable; for these reasons it is not used for *in vivo* and *in vitro* studies. [1] One of the most common artificial saliva is the Tani-Zucchi formulation [2], which, for example, was employed for the investigation of the corrosion behaviour of stainless steels for orthodontics [3] and for correlating it with the surface modifications induced on ancient brass wind instruments of historical interest when played by musicians. [4,5]

Tani-Zucchi saliva mainly contains inorganic salts, urea and α-amylase as organic compounds. In previous papers, the authors reported that, on brass alloy surfaces following the exposure of the samples to the model saliva solution, a thick surface film composed to a large extent of CuSCN and $Zn_3(PO_4)_2$ was observed. [4,5] In a recent work [6], the corrosion behaviour of CuZn37 exposed to Darvell (D) [7], Carter-Brugirard (C-B) [8] and SALMO [9] formulations was investigated by electrochemical measurements, and it was found that the corrosion rate determined after 16 hours varies in the order: D (2.3 (0.3) μm / year) > C-B (1.2 (0.2) μm / year) > SALMO (0.8 (0.2) μm / year). These three model saliva solutions were chosen from those of the literature due to their composition: all of them contain chlorides, thiocyanates, phosphates and carbonates but they differ for the content in the organic compounds: D solution contains urea, lactic acid, trisodium citrate, and uric acid; SALMO solution contains urea and glycine; C-B solution contains only urea. The influence of organic compounds on the surface chemistry of brass alloys is scarcely investigated to date. In this work the role of organic compounds in artificial saliva is investigated by X-ray photoelectron spectroscopy (XPS) in order to correlate the corrosion rate to the composition and thickness of the surface film on CuZn37 samples after the contact with the three different saliva formulations.

Experimental

A brass alloy CuZn37 supplied by Brütsch/Rüegger Werkzeuge AG, CH was chosen for testing. The composition of the alloy was determined by a hand-held standard-less-X-ray fluorescence. (XRF) spectrometer SPECTRO xSORT (Spectro Analytical Instruments GmbH, Kleve, Germany) A Rh-anode was operated applying an acceleration voltage of 50 kV. The analysis method was "precious metals". Three independent samples were analysed and the composition was found to be 64.5 (0.1) wt % copper and 35.5 (0.1) wt % zinc.
The chemical composition of D [7], C-B [8] and SALMO [9] solutions is reported in Table 1.
The brass samples, mechanically polished as described in [10] to ensure a reproducible surface, were analysed by X-ray photoelectron spectroscopy (XPS) prior to and after the exposure to the solutions in an electrochemical cell at ambient temperature (T = 298.2 ± 0.1 K). Following the contact with the solutions the brass samples were rinsed with bi-distilled water (specific conductivity = 1.1 μS cm^{-1} at 293.2 K) and dried under an argon stream.
XPS measurements: XPS spectra were acquired using a Theta Probe spectrometer (Thermo Fisher Scientific, Eat Grinstead, UK). The analyses were carried out using a monochromatic AlKα source (energy = 1486.6 eV, 100 W) selecting a spot size of 400 μm. Survey and high-resolution spectra were acquired with a step size of 1 eV and 0.05 eV respectively, in fixed analyser transmission mode (FAT). The pass energy was set at 200 eV and 100 eV for the acquisition of survey and HR spectra respectively in standard lens mode. In these conditions the full-width at half-maximum (fwhm) of the peak height for Ag $3d_{5/2}$ was found to be equal to 0.93 eV. The linearity of the binding energy scale was checked according to ISO 15472:2010 with an accuracy of ± 0.1 eV.
Data processing: Data were processed with CASA XPS software (v2.3.24, Casa Software Ldt., Wilmslow, Cheshire, UK) as described in [10]. The quantitative composition of the film was calculated starting from the experimental areas corrected for the sensitivity factors that take into account the Scofield ionization cross section [11], the asymmetry factor [12], the spectrometer transmission function [13] and the inelastic mean free path [14]. As far as copper and zinc content, on those samples where metallic and oxidized element are not distinguishable by photoelectron signals (MP, C-B and SALMO), the percentage of 2p areas ascribed to oxidised species was calculated starting from the oxidised element/metal ratios determined on the Auger signals, following the strategy developed in [10].

Results

CuZn37 mechanically polished

The XPS survey spectrum (Figure 1a) reveals the presence of the signals of Cu, Zn, belonging to the alloy, C and O due to the contact of the surface with the environment during the sample transfer to the spectrometer. The high-resolution spectra of the most intense photoelectron lines of copper and zinc show Cu $2p_{3/2}$ signal at 932.5 (0.1) eV and Zn $2p_{3/2}$ at 1021.7 (0.1) eV. As it is well known, Cu 2p and Zn 2p do not exhibit a chemical shift between Cu (0) and Cu (I), and Zn (0) and ZnO with the current level of energy resolution. However, it is possible to distinguish them exploiting the Auger signals [10, 15]. The curve fitting of $CuL_3M_{4.5}M_{4.5}$ and $ZnL_3M_{4.5}M_{4.5}$ Auger peaks were performed according to [10]. The kinetic energy of the peak assigned to Cu (0) of $CuL_3M_{4.5}M_{4.5}$ was found at 918.5 (0.1) eV, the very weak signal of the Cu (I) component at 916.7 (0.1) eV. For the $ZnL_3M_{4.5}M_{4.5}$ the metal component was found at KE 992.1 (0.1) eV, while the Zn (II) component was at 987.9 (0.1) eV. These data are in agreement with the literature [10,15-17].

The X-ray induced Auger spectra (XAES) of zinc (Figure 1b) suggest the presence of metallic and oxide components, indicating that a thin oxide layer is formed on the mechanically polished brass surface. A very small amount of oxidized copper is revealed by the XAES spectrum of copper (Figure 1c). Thus, the surface film formed after mechanical polishing is mainly composed of ZnO.

CuZn37 exposed to saliva formulations

In all three saliva solutions a visible surface film on the samples' surfaces was formed. In addition to Cu, Zn, C and O, sulphur and phosphorus signals were revealed in the survey spectra. The binding energy (BE) and the kinetic energy (KE) of the most intense photoelectron and Auger peaks are reported in Table 2. The Cu $2p_{3/2}$ signal showed a single peak at 932.5 (0.1) eV for all samples. The Zn $2p_{3/2}$ signal was found at 1021.7 (0.1) eV on brass exposed to D solution and it was assigned to Zn(0) and ZnO. Following the exposure to SALMO and C-B solutions the Zn $2p_{3/2}$ signal was revealed at 1022.9 (0.1) eV and attributed to the presence of a zinc-phosphate film [18-20]. The main component of the Zn $L_3M_{4.5}M_{4.5}$ Auger signals was located at 985.6 (0.1) eV. In the case of brass in contact with D formulation metallic zinc and oxide components were only present. The Auger signal was found at 987.8 (0.2) eV and it was assigned to ZnO according to the literature [10].
The main component in the copper Auger spectrum, Cu $L_3M_{4.5}M_{4.5}$, was found at 915.5 (0.1) eV following the exposure to SALMO and C-B. In the case of the samples exposed to D, the Cu(I) component was found at 916.0 (0.3) eV, assigned to CuSCN [4,5]. The Auger parameters α', were also calculated according to [21,22] and are listed in Table 2.
The Zn/Cu intensity ratio varies on the surfaces exposed to the different formulations: in the samples exposed to D solution it is lower than in the other cases (Table 3).
The S 2p high-resolution spectra (Figure 3a) show on all samples the presence of a signal at 163.4 (0.1) eV assigned to $^{-}$SCN. [4-5, 10, 18]
P 2p signal at 134.3 (0.1) eV attributed to a phosphate [4-5, 10, 18] was only revealed on the brass after the contact with SALMO and C-B formulations. The brass surface exposed to D solution exhibited no P but another component in the S 2p region at 161.9 (0.1) eV (Figure 3b).

Discussion

In a recent work of the authors [6], the corrosion behaviour of CuZn37 exposed to D, C-B and SALMO formulations was investigated by electrochemical measurements, and it was found that the corrosion rate varied in the order: D > C-B > SALMO. In this work the corrosion behaviour can be correlated to the surface composition of the film formed. Previous papers [4-5, 10,18] showed that the film exposed to the model saliva solution Tani-Zucchi, was mainly composed of CuSCN and $Zn_3(PO_4)_2$. Tani-Zucchi is a solution principally constituted of inorganic compounds [2] and it was concluded that the surface film was able to protect the brass surface against corrosion. The question, which remained open, was whether the presence of organic compounds might influence the composition of the surface film and its corrosion resistance. In the following the results obtained in this work are discussed.

Effect of citrate on film composition

The lowest Zn/Cu ratio (Table 3) and the absence of P 2p signal (Figure 2b) observed on the brass exposed to Darvell solution could be explained by the formation of a soluble zinc complex that might hinder the growth of insoluble protective films made of zinc-phosphate as revealed on the surface of the brass alloys in contact with SALMO and Carter-Brugirard saliva solutions (Table 3). Possible soluble complexes that might form are zinc citrate and zinc lactate. Considering the formation

constant (K_f), zinc citrate is more likely [23]. For this reason, a test with a brass sample exposed for 1h to a solution of trisodium citrate dihydrate with the same concentration of trisodium citrate in D solution [7] was performed. The Zn/Cu ratio is found about 3 times lower than the Zn/Cu ratio on mechanically polished CuZn37 (figure 4). These data might confirm the possible formation of soluble zinc-citrate complex. Moreover, the presence of the metallic component on XAES spectra of Cu and Zn indicates the presence of a very thin film. These facts could explain the high corrosion rate observed for brass exposed to D solution: the film formed was less protective than the ones formed in SALMO and C-B solutions.

Effect of uric acid

According to the literature [24] Cu (I) cation is classified as a soft Lewis acid and usually coordinates the SCN^- ion *via* sulphur atom. Additionally, SCN^- ion is known to be an ambidentate ligand: if the thiocyanate ion would be the only ligand present, its mode of bonding generally would follow the hard (M-NCS) or soft (M-SCN) principle [24]. However, the presence of other ligands might determine whether the metal behaves as a hard ion or as a soft ion resulting in different thiocyanate complexes [24-28]. On the basis of the other works of the authors, the sulphur component at 161.9 (0.1) eV might be assigned either to the formation of Cu (I) sulphide [29-31], or to the formation of a mixed complex with thiocyanate as reported for other metal ions compounds with SCN^- [32, 33] in the presence of ligands as bipyridine. The possible formation of a mixed complex was further investigated examining a pure copper sample after the contact for 1 h with a solution of sodium thiocyanate and uric acid using the same concentration as in D formulation [7]. The same experiment was repeated replacing the uric acid with lactic acid. This organic compound is also able to react with Cu(I) but it is smaller than the uric acid. Only when uric acid and NaSCN were simultaneously present, the S2p spectrum indicated the presence of the second component at 161.9 (0.1) eV (Figure 4). This result might substantiate the formation of a mixed compound between Cu(I) NCS and uric acid due to steric and electronic effects exerted by uric acid.

Conclusions

On the basis of the findings presented the following conclusions can be drawn:
The presence of thiocyanate and phosphates lead to the formation of a protective film of CuSCN and $Zn_3(PO_4)_2$ in the case of C-B and SALMO. The presence of citric acid may result in the formation of soluble zinc citrate that hinders the growth of the insoluble protective zinc-phosphate film. Furthermore, thiocyanate and uric acid in the D solution can lead to the formation not only of copper thiocyanate but also of small amount of a copper compound where copper (I) is interacting with SCN via nitrogen atom and with uric acid. The high dissolution rate measured on brass samples exposed to D solution may be explained by the presence of organic compounds leading to the formation of a thin and less protective film on the brass.
A final remark is that the choice of a model solution may be crucial when investigating the performance of materials in contact with simulated biofluids.

Acknowledgments

The Italian Ministry of University and Research (MIUR) and Regione Autonoma della Sardegna are thanked for financial support (POR FSE 2014/2020).

References

1. Pytko-Polonczyk J., Jakubik A., Przeklasa-Bierowiec A., Muszynska B., Artificial saliva and its use in biological experiments. *J. Physiol. Pharmacol*. 2017; 68:807.
2. Tani G., Zucchi F., Electrochemical measurement of the resistance to corrosion of some commonly used metals for dental prosthesis, *Minerva Stomatol*., 1967; 16: 710–713.
3. Elsener, B.; Pisu, M.; Fantauzzi, M.; Addari, D.; Rossi, A. Electrochemical and XPS surface analytical study on the reactivity of Ni-free stainless steel in artificial saliva. *Mater. Corros.* 2016; 6: 591–599.
4. Cocco F., Fantauzzi M., Elsener B., Rossi A., Dissolution of brass alloys naturally aged in neutral solutions – an electrochemical and surface analytical study, *RSC Adv.*, 2016, 6, 90654-90665.
5. Cocco F., PhD thesis, Sustainability in cultural heritage: from diagnosis to the development of innovative systems for monitoring and understanding corrosion inside ancient brass wind instruments, University of Cagliari, 2016.
6. Biggio D., Master's thesis, Effect of the composition of model solutions for brass corrosion studying, University of Cagliari, 2019.
7. Darvell B.W., The development of an artificial saliva for in vitro amalgam corrosion studies, *J. Oral Rehab.*, 1978, 5, 41-49.
8. Vitelaru, C., Ghiban, N., Parau, A.C., Balaceanu, M., Miculescu, F. and Vladescu, A., Corrosion behaviour of Ti6Al4V alloy in artificial saliva solution. *Mat.-wiss. u. Werkstofftech*., 2014, 45: 91-98.
9. Crea F., De Stefano C., Milea D., Pettignano A., Sammartano S., SALMO and S3M: A Saliva Model and a Single Saliva Salt Model for Equilibrium Studies, *Bioinorg. Chem. Appli.*, 2015; 2015: Article ID 267985
10. Cocco F., Elsener B., Fantauzzi M., Atzei D., Rossi A., Nanosized surface films on brass alloys by XPS and XAES, *RSC Adv.*, 2016; 6: 31277-31289.
11. Scofield J. H., Hartree-Slater subshell photoionization cross-sections at 1254 and 1487 eV, *J. Electron Spectrosc. Relat. Phenom*., 1976; 8: 129–137.
12. Reilman RF, Msezane A., Manson S.T., Relative intensities in photoelectron spectroscopy of atoms and molecules, *J. Electron. Spectrosc. Relat. Phenom.*, 1976; 8:389–394.
13. Fantauzzi M., Pacella A., Fournier J., Gianfagna A., Andreozzi G. B., Rossi A., Surface chemistry and surface reactivity of fibrous amphiboles that are not regulated as asbestos, *Anal. Bioanal. Chem.,* 2012; 404: 821–833.
14. Seah M. P., Dench W. A., Quantitative electron spectroscopy of surfaces: A standard data base for electron inelastic mean free paths in solids, *Surf. Interface Anal.*, 1979; 1: 2-11.
15. Biesinger M. C., Lau Leo W.M., Gerson Andrea R., Smart Roger St.C., Resolving surface chemical states in XPS analysis of first row transition metals, oxides and hydroxides: Sc, Ti, V, Cu and Zn, *Appl. Surf. Sci.*, 2010; 257: 887–898.
16. NIST Standard Reference Database 20 Version 4.1, http://srdata.nist.gov/xps.
17. Moulder J. F., Stickle W. F., Sobol P. E and Bomben K. D., Handbook of X-ray Photoelectron Spectroscopy, Perkin-Elmer Corp., *Physical electronics*, Minnesota, 1992.
18. Fantauzzi M, Elsener B., Cocco F., Passiu C. and Rossi A., Model Protective Films on Cu-Zn Alloys Simulating the Inner Surfaces of Historical Brass Wind Instruments by EIS and XPS, *Front. Chem*., 2020; 8:272.

19. Crobu M., Rossi A., Mangolini F., Spencer ND. Chain-length-identification strategy in zinc polyphosphate glasses by means of XPS and ToF-SIMS. *Anal. Bioanal. Chem*. 2012;403:1415-1432.
20. Crobu M., Rossi A., Spencer N.D., Effect of Chain-Length and Countersurface on the Tribochemistry of Bulk Zinc Polyphosphate Glasses, *Tribol. Lett.*, 2012; 48:393-406.
21. Wagner C.D., Chemical shifts of Auger lines, and the Auger parameter, *Faraday Discuss. Chem. Soc.*, 1975; 60: 291-300.
22. Moretti G., Auger parameter and Wagner plot in the characterization of chemical states by X-ray photoelectron spectroscopy: a review., *J. Electron. Spectr. Related Phenom*. 1998; 95: 95-144.
23. Krężel A, Maret W. The biological inorganic chemistry of zinc ions. *Arch. Biochem. Biophys*. 2016; 611: 3-19.
24. Pearson R. G., Chemical Hardness. *Wiley-VCH Verlag GmbH*, Weinheim, 1997.
25. Burmeister J., Ambidentate ligands, the schizophrenics of coordination chemistry, *Coord. Chem. Rev.*,1990; 105: 77-133.
26. Aldakov D., Chappaz-Gillot C., Salazar R., Delaye V., Welsby K. A., Ivanova V., Dunstand P.R., Properties of Electrodeposited CuSCN 2D Layers and Nanowires Influenced by Their Mixed Domain Structure. *J. Phys. Chem. C*, 2014, 118(29), 16095-16103.
27. Meek D.W., Nicpon P. E., Imhof Meek V., Mixed Thiocyanate Bonding in Palladium (II) Complexes of Bidentate Ligands,*J. Am. Chem. Soc.*, 1970; 92: 5351-5359.
28. Gholivand K., Farshadfar K., Roe S. M., Hosseini M. and Gholami A., Investigation of structure-directing interactions within copper(I) thiocyanate complexes through X-ray analyses and non-covalent interaction (NCI) theoretical approach, *Cryst .Eng. Comm.*, 2016; 18: 7104-7115.
29. Fantauzzi, M., Elsener, B., Atzei, D., Lattanzi, P. and Rossi, A., The surface of enargite after exposure to acidic ferric solutions: an XPS/XAES study, *Surf. Interface Anal*., 2007, 39: 908–915.
30. Fantauzzi M., Rigoldi A., Elsener B., Atzei D., Rossi A. A contribution to the surface characterization of alkali metal sulfates, *J. Electron Spectrosc. Relat. Phenom., 2014:* 193: 6–15.
31. Fantauzzi M., Rossi G., Elsener B., Loi G., Atzei D., Rossi A., An XPS analytical approach for elucidating the microbially mediated enargite oxidative dissolution, *Anal. Bioanal. Chem.*, 2009, 393: 1931–1941.
32. Walton R.A., X-ray Photoelectron Spectra of Inorganic Molecules [11]. XXIII. On the Question of the Usefulness of XPS in Studying the Ambidentate Nature of the Thiocyanate Liiand, *Inorg. Chim. Acta*, 1979; 37: 231-240.
33. Bowmaker Graham A. and Hanna John V. Z., IR Spectroscopy of Two Polymorphs of Copper(I) Thiocyanate and of Complexes of Copper(I) Thiocyanate with Thiourea and Ethylenethiourea, *Z. Naturforschung,* 2009; 64b: 1478–1486.

Table 1: Composition of the model solutions: Darvell (D), Carter-Brugirard (C-B) and SALMO.

Anions	**Concentration (mmol / dm^3)**		
	D	**C-B**	**SALMO**
Cl^-	29.8	28.1	25.3
$H_2PO_4^-$ & HPO_4^{2-}	4.7	3.2	8.5
HCO_3^-	7.1	17.9	11.4
SCN^-	2.5	3.4	2.0
F^-	-	-	0.0025
OH^-	0.1	-	-
SO_4^{2-}	-	-	1.1
Organics	1.4 (**Citrate, lactic acid, urea, uric acid**)	2.2 (**Urea**)	3.6 (**Urea, glycine**)

Table 2 : Average binding energy (BE) of the most intense photoelectron peaks, kinetic energy of Auger peaks of the elements detected on CuZn37 surface after 1h of exposure at Darvell (D), Carter-Brugirard (C-B) and SALMO saliva model solutions. Auger parameters (α' = BE + KE) of Zn and Cu are reported. Standard deviations are given in parentheses.

CuZn37	**D 1h**		**C-B 1h**		**SALMO 1h**	
	BE (eV)		**BE (eV)**		**BE (eV)**	
C 1s ($^{-}$SCN)	285.8 (0.1)		286.0 (0.1)		286.1 (0.1)	
Cu $2p_{3/2}$	932.5 (0.1)		932.5 (0.1)		932.5 (0.1)	
N1s	398.7 (0.1)		398.7 (0.1)		398.7 (0.1)	
N1s	400.2 (0.1)		400.2 (0.1)		400.2 (0.1)	
O1s	530.8 (0.2)		531.6 (0.1)		531.7 (0.2)	
O1s	532.0 (0.1)		532.5 (0.1)		532.5 (0.1)	
O1s	533.2 (0.3)		533.4 (0.2)		533.9 (0.2)	
S $2p_{3/2}$ ($^{-}$SCN)	163.2 (0.1)		163.5 (0.1)		163.5 (0.1)	
S 2p (II)	161.9 (0.1)		-		-	
P $2p_{3/2}$	-		134.2 (0.1)		134.4 (0.1)	
Zn$2p_{3/2}$	1021.7 (0.2)		1022.9 (0.1)		1022.9 (0.1)	
	KE (eV)	**α'**	**KE (eV)**	**α'**	**KE (eV)**	**α'**
Cu $L_3M_{4,5}M_{4,5}$ film	916.0 (0.3)	1848.5 (0.2)	915.5 (0.1)	1848.0 (0.1)	915.5 (0.1)	1848.0 (0.1)
Zn $L_3M_{4,5}M_{4,5}$ film	987.8 (0.2)	2009.5 (0.3)	985.7 (0.1)	2008.6 (0.1)	985.4 (0.1)	2008.3 (0.1)

Table 3: Quantitative composition (at %) of the main elements detected and Zn / Cu ratio on CuZn37 surface after 1h of exposure at Darvell (D), Carter-Brugirard (C-B) and SALMO saliva model solutions. Standard deviations are given in parentheses.

CuZn37	**D 1h**	**C-B 1h**	**SALMO 1h**
	at %	**at %**	**at %**
C 1s ($^{-}$SCN)	19 (1)	14.8 (0.3)	13.4 (0.4)
Cu $2p_{3/2}$ film	28 (2)	10.0 (0.6)	12.4 (0.4)
N1s	13 (2)	7.4 (0.5)	8.7 (0.4)
N1s	2.1 (0.5)	0.7 (0.2)	0.7 (0.2)
O1s	12 (2)	32 (1)	31.3 (0.4)
S $2p_{3/2}$ ($^{-}$SCN)	17 (3)	12.0 (0.5)	14.1 (0.5)
S 2p (II)	5 (2)	-	-
P $2p_{3/2}$	-	7.4 (0.4)	7 (1)
Zn$2p_{3/2}$ film	4 (1)	15 (1)	12.0 (0.6)
	D 1h	**C-B 1h**	**SALMO 1h**
Zn film / Cu film	0.15 (0.03)	1.5 (0.2)	0.97 (0.07)

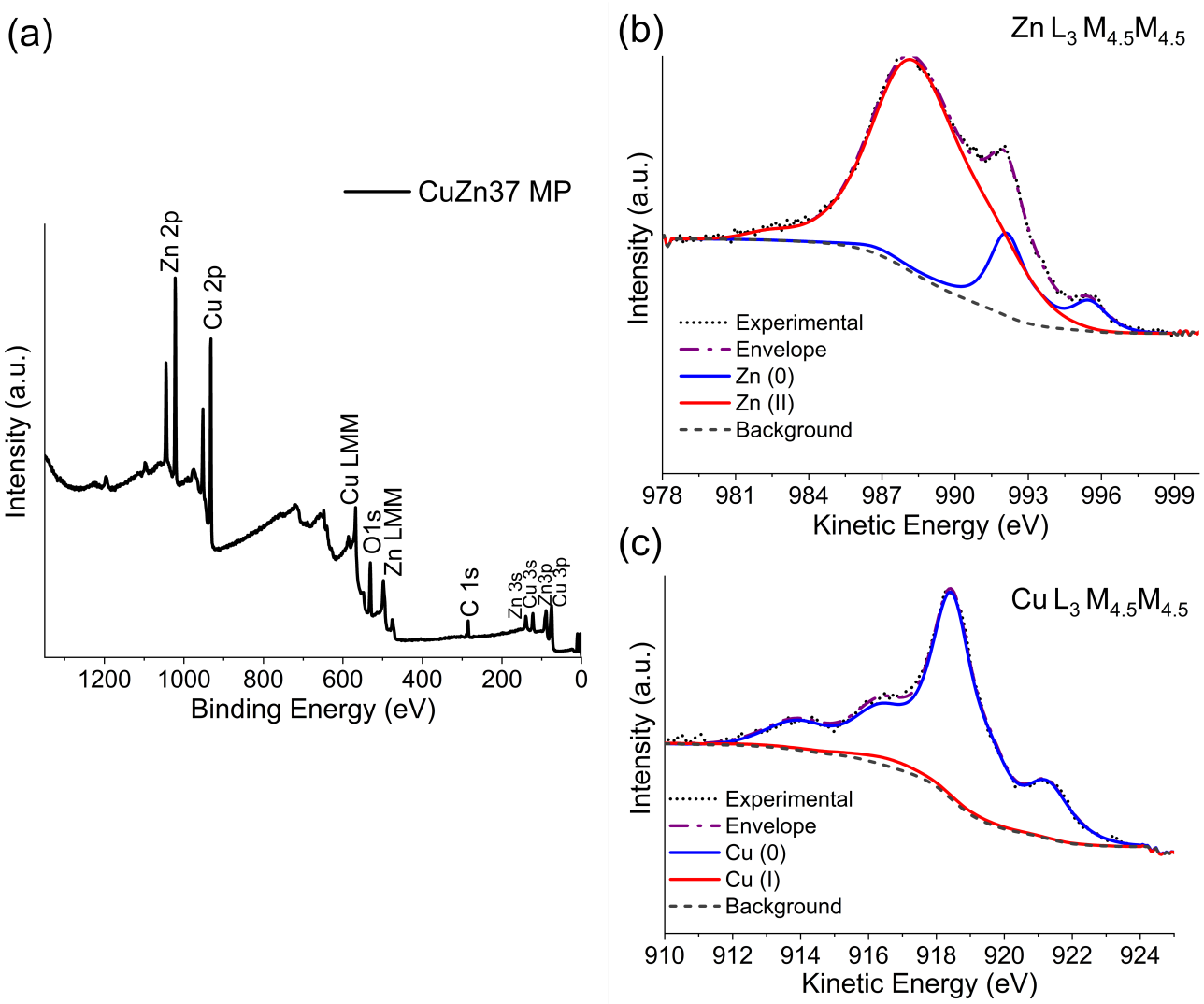

Figure 1 : a) Survey spectrum of mechanically polished CuZn37. b) X-ray induced Auger spectra (XAES) of $ZnL_3M_{4,5}M_{4,5}$ and c) Cu $L_3M_{4,5}M_{4,5}$ of mechanically polished CuZn37.

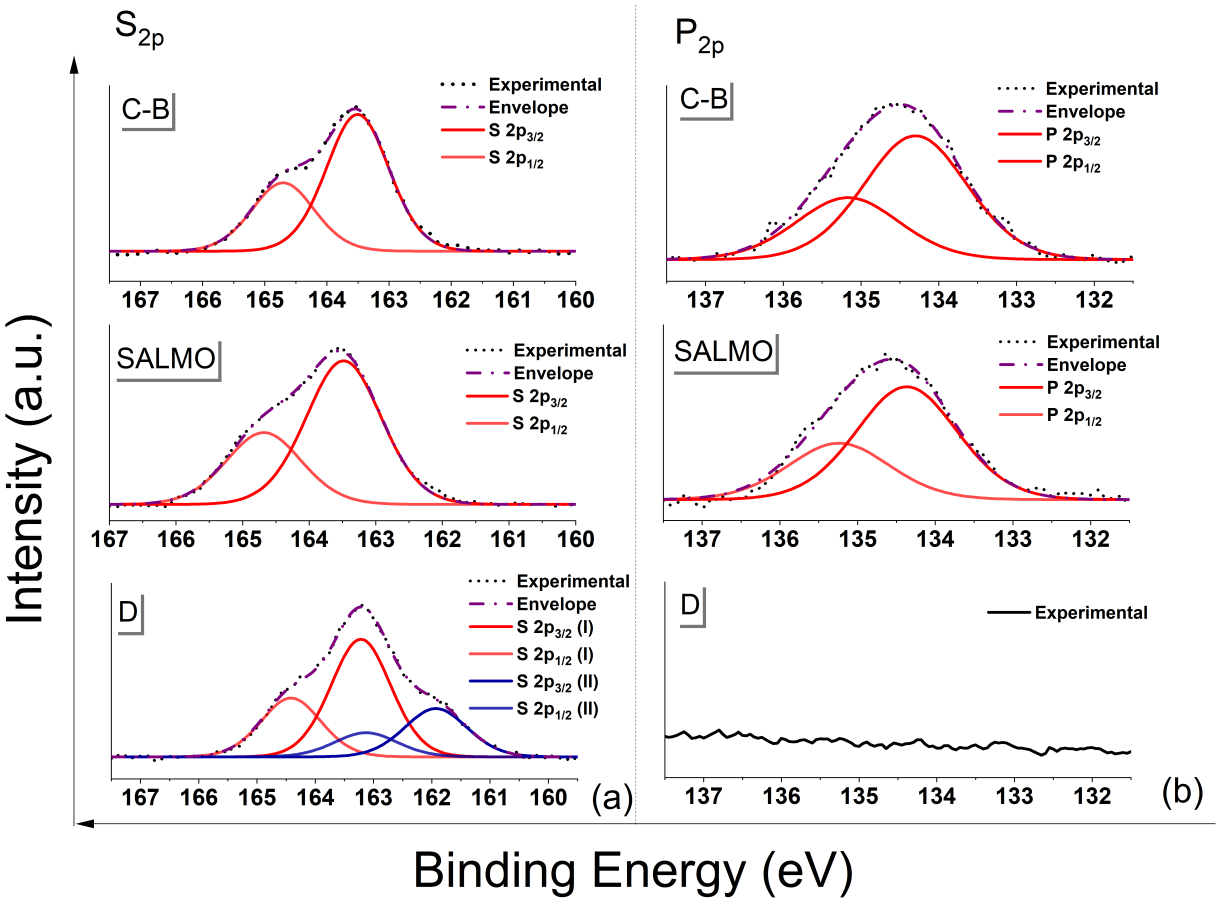

Figure 2: a) High-resolution spectra of S2p and b) P2p of CuZn37 after 1 h of contact with (top to bottom) Carter-Brugirard (C-B), SALMO and Darvell (D) formulations.

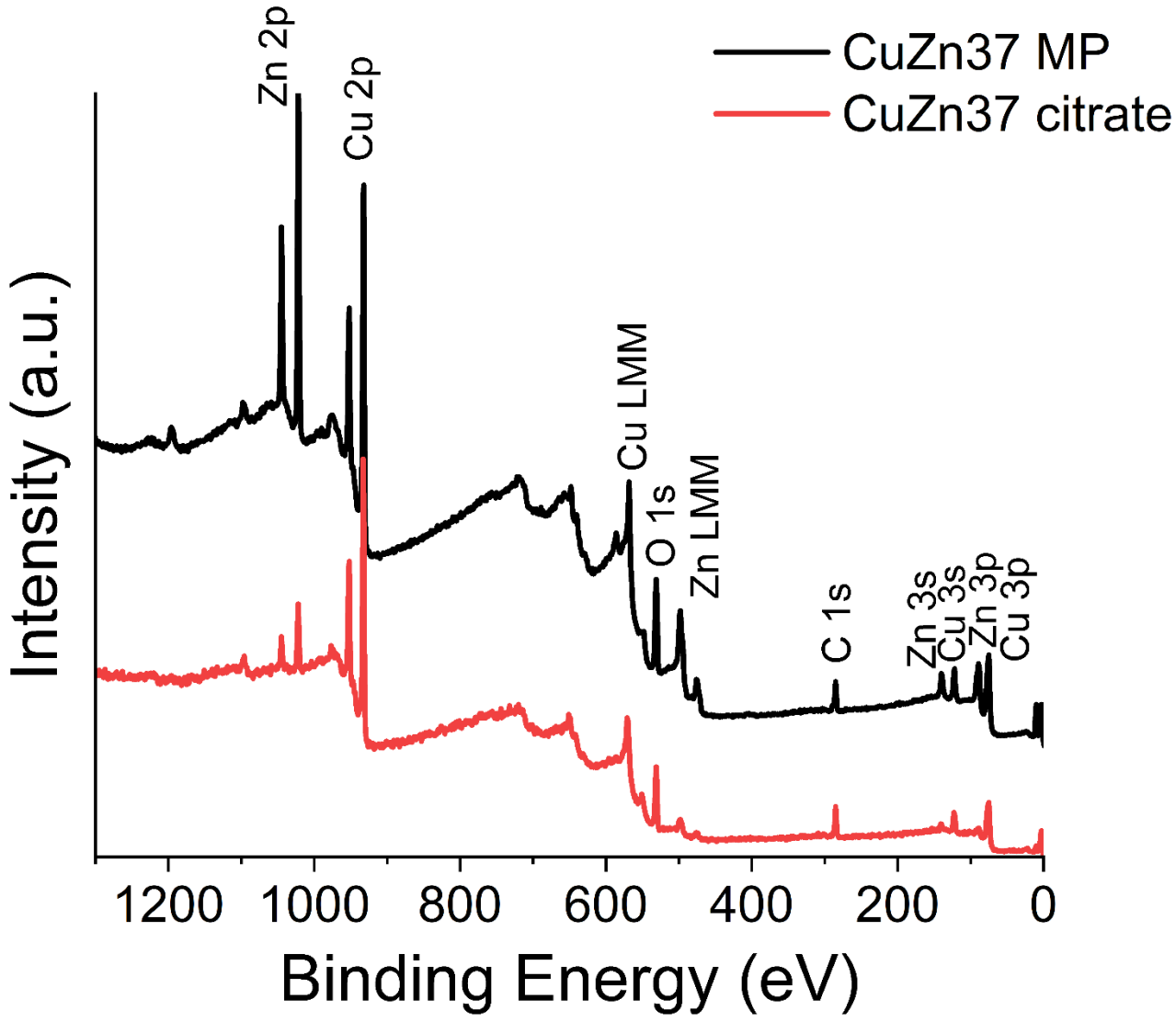

Figure 3: Survey spectra of mechanically polished (MP) CuZn37 and CuZn37 samples after exposure for 1h to trisodium citrate solution. The Zn/Cu ratio on brass exposed to citrate solution is three times lower than Zn/Cu on MP brass.

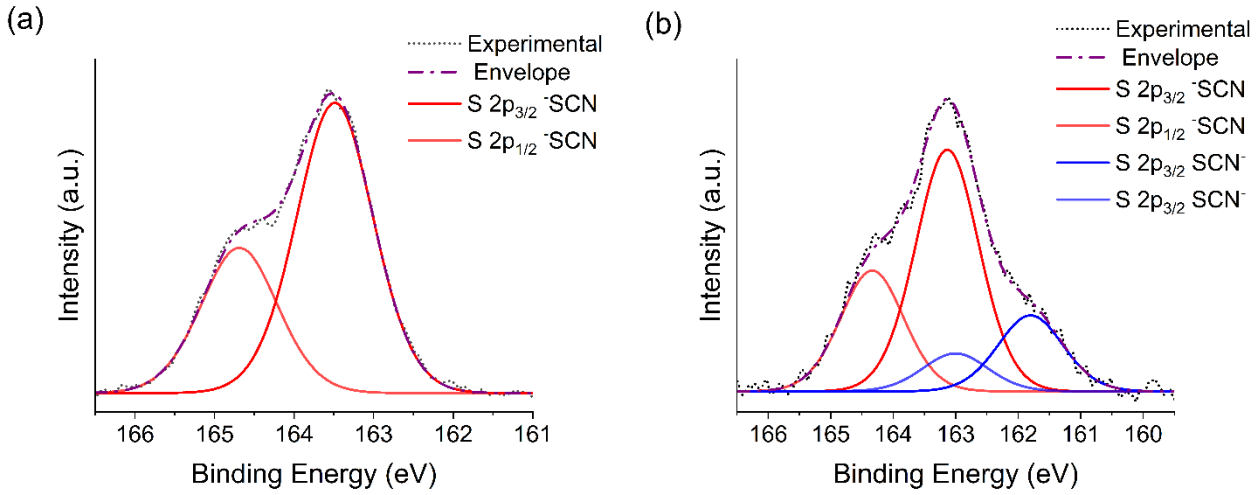

Figure 4: High-resolution spectra of S2p signal of a) pure copper in contact with NaSCN (0.20 g / dm^3) and lactic acid (0.07 g / dm^3) solution and b) pure copper in contact NaSCN (0.20 g / dm^3) and uric acid (15 mg / dm^3) solution.